JACS
JOURNAL OF THE AMERICAN CHEMICAL SOCIETY

ARTICLE

pubs.acs.org/JACS

Fluorescence Probe for Lysophospholipase C/NPP6 Activity and a Potent NPP6 Inhibitor†

Mitsuyasu Kawaguchi,[‡,§] Takayoshi Okabe,[⊥] Shinichi Okudaira,[#] Kenjiro Hanaoka,[‡,§] Yuuta Fujikawa,[‡,§] Takuya Terai,[‡,§] Toru Komatsu,[‡,§] Hirotatsu Kojima,[§,⊥] Junken Aoki,[#] and Tetsuo Nagano*[,‡,§,⊥]

[‡]Graduate School of Pharmaceutical Sciences, The University of Tokyo, 7-3-1 Hongo, Bunkyo-ku, Tokyo 113-0033, Japan

[§]CREST, JST, Sanbancho-blg, 5 Sanbancho, Chiyoda-ku, Tokyo, 102-0075, Japan

[⊥]Chemical Biology Research Initiative, The University of Tokyo, 7-3-1 Hongo, Bunkyo-ku, Tokyo 113-0033, Japan

[#]Graduate School of Pharmaceutical Sciences, Tohoku University, 6-3 Aoba Aramaki, Aoba-ku, Sendai, Miyagi 980-8578, Japan

Supporting Information

ABSTRACT: Nucleotide pyrophosphatases/phosphodiesterases (NPPs) are ubiquitous membrane-associated or secreted ectoenzymes that have a role in regulating extracellular nucleotide and phospholipid metabolism. Among the members of the NPP family, NPP1 and -3 act on nucleotides such as ATP, while NPP2, -6, and -7 act on phospholipids such as lysophosphatidylcholine and sphingomyelin. NPP6, a recently characterized NPP family member, is a choline-specific glycerophosphodiester phosphodiesterase, but its functions remain to be analyzed, partly due to the lack of highly sensitive activity assay systems and practical inhibitors. Here we report synthesis of novel NPP6 fluorescence probes, TG-mPC and its analogues TG-mPC$_3$C, TG-mPC$_5$C, TG-mPENE, TG-mPEA, TG-mPhos, TG-mPA, TG-mPMe, and TG-mPPr. Among the seven NPPs, only NPP6 hydrolyzed TG-mPC, TG-mPC$_3$C, and TG-mPENE. TG-mPC was hydrolyzed in the cell lysate from NPP6-transfected cells, but not control cells, showing that it is suitable for use in cell-based NPP6 assays. We also examined the usefulness of TG-mPC as a fluorescence imaging probe. We further applied TG-mPC to carry out high-throughput NPP6 inhibitor screening and found several NPP6-selective inhibitors in a library of about 80 000 compounds. Through structure−activity relationship (SAR) analysis, we identified a potent and selective NPP6 inhibitor with an IC$_{50}$ value of 0.21 μM. Our NPP6-selective fluorescence probe, TG-mPC, and the inhibitor are expected to be useful to elucidate the biological function of NPP6.

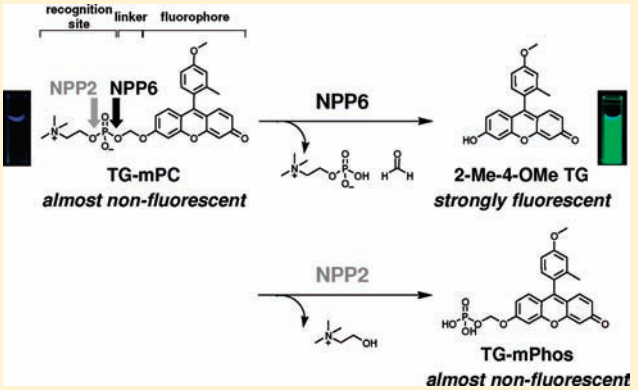

INTRODUCTION

Nucleotide pyrophosphatases/phosphodiesterases (NPPs) are ubiquitous membrane-associated or secreted ectoenzymes that have roles in regulating extracellular levels of nucleotides, such as ATP and ADP, and phospholipids, such as lysophosphatidylcholine (LPC) and sphingomyelin (SM).[1−4] The mammalian NPP family consists of seven members (NPP1−7), which are divided into two subgroups, NPP1−3 (type II membrane proteins) and NPP4−7 (type I membrane proteins), based on their primary structure (see Supporting Information Figure S1A).[1−4] Among NPP family members, NPP1 regulates the extracellular phosphate levels by hydrolyzing nucleotide substrates, such as ATP, thereby modulating bone formation, insulin receptor signaling, and type 2 diabetes.[5−13] NPP2/Autotaxin is identical to lysophospholipase D (lysoPLD) and has key roles in various pathophysiological processes such as angiogenesis, development of neuropathic pain, lymphocyte trafficking, and tumor cell invasion.[14−19] Fluorescence probes for NPP2, such as CPF4 and FS-3 were developed recently, and a number of NPP2 inhibitors were identified using these NPP2-specific probes.[20−30] By contrast, the roles of NPP4−7 have not been determined in detail.[3] Isoform-specific fluorescence probes and inhibitors would be useful for this purpose.

NPP6/lysoPLC is a choline-specific glycerophosphodiester phosphodiesterase and is dominantly expressed in brain and kidney, especially in proximal tubules. Its natural substrates are choline-containing glycerophosphodiesters, such as lysophosphatidylcholine (LPC) and glycerophosphorylcholine (GPC).[3] It has been suggested that NPP6 is important for the reuptake of physiologically essential choline in kidney and also in brain development. Furthermore, Cravatt et al. reported that NPP6, in addition to fatty acid amide hydrolase (FAAH), metabolizes phosphorylcholine *N*-acylethanolamines

Received: February 9, 2011
Published: July 01, 2011

ACS Publications © 2011 American Chemical Society

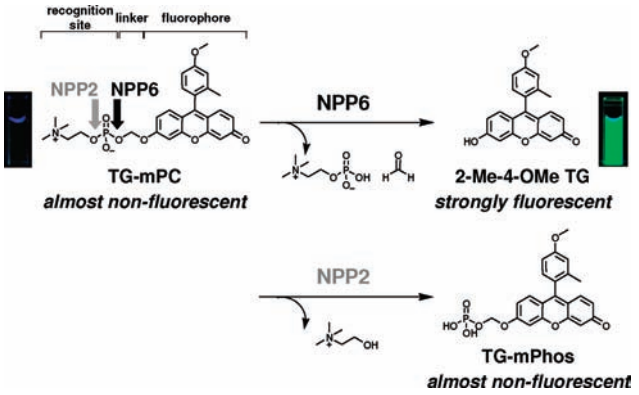

Figure 1. Strategy to selectively detect NPP6 activity. TG-mPC consists of three moieties: NPP6 recognition moiety, linker moiety, and fluorophore. TG-mPC is almost nonfluorescent before enzymatic reaction. NPP6 (cleavage site shown by black arrow) generates strongly fluorescent 2-Me-4-OMe TG with elimination of phosphorylcholine and formaldehyde (upper scheme). On the other hand, NPP2 (cleavage site shown by shadowed arrow) generates almost nonfluorescent TG-mPhos with the elimination of a choline (bottom scheme).

(PC-NAE) in brain.[31] Highly sensitive activity sensors and potent inhibitors of NPP6 would be useful to establish the function of NPP6 in more detail. In addition, many kinds of high-throughput screening (HTS) systems employing fluorescence probes have been used to discover small-molecular inhibitors of a variety of targets. This methodology is extremely useful for the identification of novel inhibitors from large chemical libraries, not only as candidate therapeutic agents but also as chemical tools for functional studies of the targets, because of the high sensitivity of fluorescence-based HTS, compared with classical absorption-based assay.[32] For example, a recently developed fluorescence probe for NPP2/ATX, CPF4, was used to discover NPP2/ATX inhibitors[20] and was also employed in biochemical characterization of ATX.[21] So, in this study, we report the development of a novel NPP6-selective fluorescence probe, TG-mPC, and the discovery of a potent and selective NPP6 inhibitor by means of screening with the use of this probe. Although many fluorescence probes targeting phospholipases have been developed, no previously reported probe can distinguish between the enzymatic activities of lysoPLC and lysoPLD.[22,33,34] Herein, we have employed a novel design strategy to obtain TG-mPC, which can clearly distinguish between the activities of lysoPLC and lysoPLD.

RESULTS AND DISCUSSION

Design of NPP6-Selective Probe. We designed 2-Me-4-OMe TokyoGreen-methyleneoxy phosphorylcholine (TG-mPC) as an NPP6-selective probe (Figure 1). TG-mPC consists of three moieties; an NPP6 recognition moiety, a linker moiety, and a fluorophore moiety. Phosphorylcholine was selected as the NPP6 recognition moiety, and oxymethylene as the linker moiety, which serves to reduce steric hindrance between the fluorophore and NPP6, and to enhance the stability of 2-Me-4-OMe TokyoGreen-methyleneoxy phosphate (TG-mPhos) and TG-mPC.[35,36] The oxymethylene linker is eliminated as formaldehyde during the hydroxylation of phosphorylcholine by NPP6. As the fluorophore moiety, we selected TokyoGreen (TG).[37] TG is an excellent fluorophore which has favorable chemical properties, including high water solubility and strong fluorescence. Further, the fluorescence properties of TG can be easily controlled by the photoinduced electron transfer (PeT) mechanism.[37] Therefore, TG is widely used as a scaffold for off/on type fluorescence probes, as in TG-βgal and TG-Phos for detection of β-galactosidase and alkaline phosphatase (ALP), respectively.[38,39]

Strategy To Detect NPP6 Activity. Our strategy to selectively detect NPP6 activity is shown in Figure 1. Our probe, TG-mPC, is almost nonfluorescent owing to the operation of the acceptor-PeT (a-PeT) mechanism.[37] However, 2-Me-4-OMe TG, a possible product of lysoPLC/NPP6 reaction, is fully fluorescent. In contrast, TG-mPhos, a possible product of lysoPLD reaction mediated by NPP2/ATX, is almost nonfluorescent. It is possible that TG-mPC would be hydrolyzed by NPP2 (cleavage at the position indicated by a shadowed arrow in Figure 1), generating TG-mPhos, but because TG-mPhos is almost nonfluorescent, we speculated that TG-mPC would be able to selectively detect NPP6 activity as a fluorescence enhancement.

Synthesis of TG-mPC. We synthesized TG-mPC in five steps (Scheme 1). Compound **2** was synthesized according to the reported method.[40] This structure was an intermediate in the synthesis of a water-soluble prodrug with a phosphate group.[41,42] Compound **2** was considered useful because it has high reactivity toward phenolic groups and is stable.

Characteristics of TG-mPC. Photochemical properties of TG-mPhos, TG-mPC, and 2-Me-4-OMe TG are summarized in Table 1. The fluorescence quantum yield (Φ_{Fl}) of TG-mPC took a quite low value (Φ_{Fl} = 0.009), whereas that of 2-Me-4-OMe TG was high (Φ_{Fl} = 0.84). TG-mPhos, the product expected to be generated by the reaction with NPP2, also showed a low value (Φ_{Fl} = 0.012). Thus, it is expected that detection of NPP6 activity is possible as a result of the strong fluorescence enhancement, whereas hydrolysis of TG-mPC by NPP2 would not result in fluorescence enhancement.

Reactivity of TG-mPC with NPPs. We examined the reactivity of TG-mPC with each NPP (NPP1−7) recombinant protein (Figure 2A,B) and found that TG-mPC is an NPP6-selective fluorescence probe in in vitro assay: fluorescence enhancement ($Fl_{3\ min}/Fl_{0\ min}$) was observed only when TG-mPC was mixed with NPP6. The value of fluorescence enhancement was 165-fold for NPP6, with much lower values for other NPPs. Using colorimetric substrates, such as pNP-TMP and pNPPC, we have been able to discriminate various NPP activities to some extent (see Supporting Information Figure S1B,C). It should be noted that TG-mPC can distinguish NPP6 and NPP7, which could not be discriminated by using colorimetric substrates. We confirmed that the product generated by enzymatic reaction with NPP6 is 2-Me-4-OMe TG by means of HPLC (see Supporting Information Figure S3). We also examined whether TG-mPC is hydrolyzed by other NPPs to form nonfluorescent TG-mPhos and found that this was not the case (see Supporting Information Figures S4,5). Because formaldehyde is generated as a byproduct, we tested whether formaldehyde affects the NPP6 activity; even at 10 μM, formaldehyde had no influence on the enzymatic activity of NPP6 (see Supporting Information Figure S6). As shown in Figure 2C and Figure S13 (see Supporting Information), TG-mPC was not hydrolyzed by porcine liver esterase (PLE), alkaline phosphatase (ALP), or acetylcholinesterase (AchE), further confirming its selectivity for NPP6.

Scheme 1. Synthesis of TG-mPC[a]

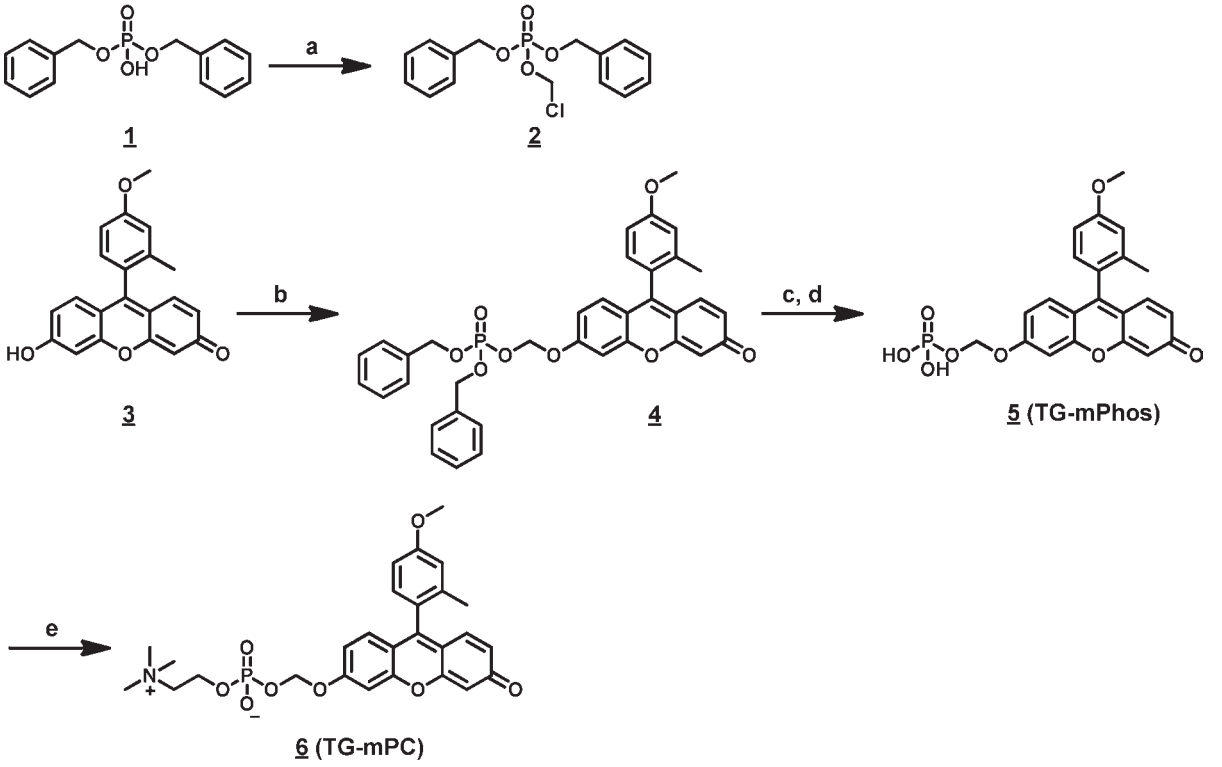

[a] Reagents and conditions: (a) chloromethyl chlorosulfate, *n*-Bu_4NHSO_4, $NaHCO_3$, CH_2Cl_2/H_2O, 0 °C to rt, 67%; (b) **2**, Cs_2CO_3, DMF, rt, 43%; (c) Pd/C, MeOH/CH_2Cl_2, rt; (d) chloranil, CH_2Cl_2/H_2O, rt, 24% in two steps; (e) bromocholine bromide, DIEA, DMF, 50 °C, 17%.

TG-mPC Analogues: Reactivity and Specificity. We synthesized various TG-mPC analogues and examined their reactivity and specificity toward various NPPs, including NPP6 (Figure 3 and see Supporting Information Scheme S1). As shown in Figure 3 and Figure S7 (see Supporting Information), at the concentration of 1 μM, NPP6 hydrolyzed TG-mPC, TG-mPC_3C, TG-mPC_5C, TG-mPENE, and TG-mPEA. The rank order is TG-mPC > TG-mPENE = TG-mPC_3C > TG-mPC_5C = TG-mPEA. NPP2, on the other hand, showed low activity toward these substrates; NPP2 weakly hydrolyzed TG-mPEA, TG-mPhos, TG-mPA, TG-mPMe, and TG-mPPr, affording a modest fluorescence increment. The TG-mPC analogues did not show any fluorescent increment with the other NPPs, i.e., NPP1, -3, -4, -5, and -7. We further examined the specificity of TG-mPC analogues for NPP6 and NPP2 using different concentrations of each substrate. The analyses revealed that TG-mPC, TG-mPC_3C, and TG-mPENE are highly selective probes for NPP6 over NPP2. TG-mPC_3C and TG-mPC_5C have a trimethylammonium group but have different linker lengths from TG-mPC, while TG-mPENE and TG-mPEA have different substituents of the amino group from TG-mPC (cationic moiety). TG-mPhos and TG-mPA have anionic structures (anionic moiety), and TG-mPMe and TG-mPPr have alkyl chains (neutral moiety). These results indicate that N-substituents of ethylamine (especially, quaternary > tertiary > primary amine) are important for selective reactivity with NPP6. In addition, the results suggest that the linker length between phosphate group and the trimethylammonium group is critical to the affinity for NPP6. These results support biochemical indications that NPP6 strongly requires a choline partial structure in its substrates.[3] TG-mPMe and TG-mPPr had higher reactivity with NPP2 than NPP6, so that TG-mPMe and TG-mPPr may be applicable to NPP2 activity assay.

Table 1. Photochemical Properties of TG-mPhos, TG-mPC, TG-Phos, and 2-Me-4-OMe TG[a]

compound	absorption maximum (nm)	extinction coefficient ($\times 10^4$ M^{-1} cm^{-1})	emission maximum (nm)	fluorescence quantum yield (Φ_{Fl})
TG-mPhos	454	1.6	511	0.012
TG-mPC	451	1.7	511	0.009
2-Me-4-OMe TG	492	8.5	511	0.84

[a] Data were measured in sodium phosphate buffer (pH 7.4). For determination of the fluorescence quantum yield, fluorescein in aq 0.1 N NaOH (Φ_{Fl} = 0.85) was used as a fluorescence standard.

Kinetic Study of TG-mPC and TG-mPC_3C. Next, we determined the kinetic parameters of TG-mPC and TG-mPC_3C. The K_m and k_{cat} values for TG-mPC and known substrates are shown in Table 2. The K_m and k_{cat} values of TG-mPC for NPP6 were 8.7 μM and 28 s^{-1}, respectively, and those of *p*-nitrophenylphosphorylcholine (pNPPC), a classical NPP6 substrate, were 11.5 μM and 14 s^{-1}. This result indicates that TG-mPC has approximately the same reactivity as pNPPC, while TG-mPC_3C has a lower affinity for NPP6 (K_m = 32.3 μM) than does TG-mPC. Moreover, TG-mPC has a much lower affinity for NPP2 than does CPF4, a classical NPP2 fluorescent

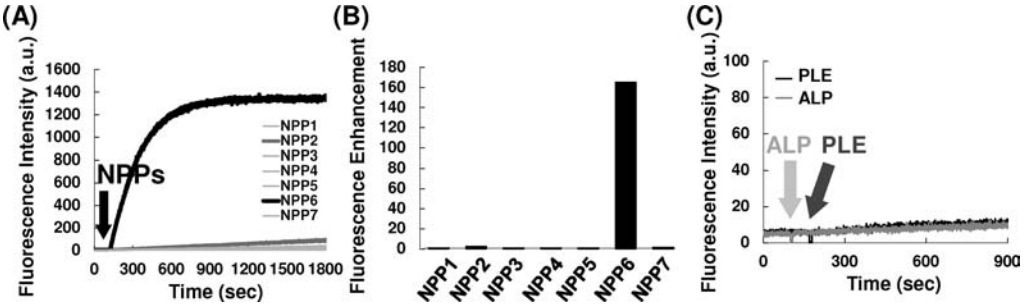

Figure 2. Reactivity of TG-mPC with NPPs and other hydrolases. (A) Time course of enzymatic reaction of TG-mPC (1 μM) with various recombinant NPPs. NPPs were added at 120 s. Reactions were performed in NPP buffer (100 mM Tris-HCl (pH 9.0), containing 500 mM NaCl, 5 mM $MgCl_2$, and 0.05% Triton-X100) at 37 °C. Bold black and deep gray lines indicate NPP6 and NPP2, respectively. Excitation and emission wavelengths were 490 and 510 nm, respectively. (B) Fluorescence enhancement ($Fl_{3\ min}/Fl_{0\ min}$) was calculated from the result in A. The reaction up to 3 min was linear. (C) Cross-reactivity of TG-mPC (1 μM) with porcine liver esterase (PLE) 5 units/mL or alkaline phosphatase (ALP). ALP or PLE was added at 120 and 180 s, respectively.

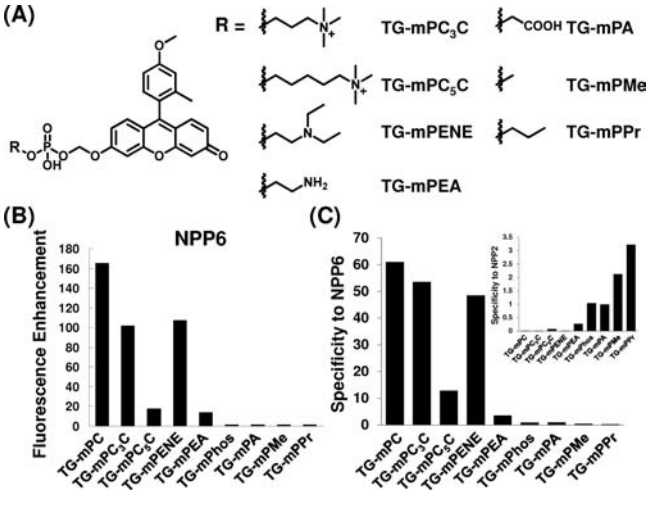

Figure 3. Reactivity and specificity of TG-mPC analogues toward NPP6. (A) Structures of TG-mPC analogues, TG-mPC$_3$C, TG-mPC$_5$C, TG-mPENE, TG-mPEA, TG-mPA, TG-mPMe, and TG-mPPr. (B) Reactivity of TG-mPC analogues with recombinant NPP6. The values of fluorescence enhancement ($Fl_{3\ min}/Fl_{0\ min}$ at 510 nm after the addition of NPPs) are shown. For details, see Supporting Information Figure S7. (C) Specificity for NPP6 against NPP2. The values of fluorescence enhancement of NPP6/NPP2 ($FI_{3\ min/0\ min}$ (NPP6)/$FI_{27\ min/0\ min}$ (NPP2) at 510 nm) are shown. Inset: specificity for NPP2 against NPP6.

substrate (see Supporting Information Figure S8). These results clearly demonstrate that TG-mPC is a selective substrate for NPP6.

Cell-Based Application. We tested the suitability of TG-mPC for cell-based assay. First, we incubated TG-mPC in cell lysates prepared from NIH3T3 cells expressing NPP6 and from control NIH3T3 cells. TG-mPC showed a fluorescence increment in NPP6 (+) cell lysate but not in NPP6 (−) cell lysate (Figure 4A). We also applied TG-mPC to the cell cultures. Significant fluorescent increment was observed when TG-mPC was added to media of NPP6-expressing NIH3T3 cells but not control NIH3T3 cells (Figure 4B). These results indicate that TG-mPC is hydrolyzed only by NPP6 among the cellular enzymes. Further, we examined whether or not TG-mPC is suitable to visualize NPP6 activity at the cellular level. HeLa cells expressing NPP6 were incubated with 10 μM TG-mPC and TG-mPPr, and fluorescence images were captured for 3 min after adding each probe. As shown in Figure 4C, the fluorescence intensities of NPP6 (+) HeLa cells and the surrounding medium were increased with TG-mPC, while there was no increase in the case of NPP6 (−) cells or when TG-mPPr was used in NPP6 (+) cells. The fluorescence of NPP6 (+) cells was significantly increased compared with NPP6 (−) cells (Figure 4D). These results indicate that TG-mPC is suitable for cell-based assay.

Table 2. K_m and k_{cat} values of TG-mPC, TG-mPC$_3$C, and pNPPC toward NPP6 and Those of TG-mPC and CPF4 toward NPP2 (for details, see Supporting Information Figure S6)

	NPP6			NPP2	
	TG-mPC	TG-mPC$_3$C	pNPPC	TG-mPC	CPF4
K_m (μM)	8.7	32.3	11.5	>400[a]	45.0
k_{cat} (sec^{-1})	28	57	14	~7.3	14

[a] This value was too large to calculate. Details are shown in Figure S8 (see Supporting Information).

Screening of NPP6 Inhibitors and Evaluation. Using TG-mPC as a substrate, we next performed NPP6 inhibitor screening of a chemical library containing about 80 000 compounds. The initial screening identified 19 compounds showing inhibitory activity (>50% at 10 μM concentration). The compounds were further tested in a second cycle of NPP6 assay, and 16 out of 19 were confirmed to inhibit NPP6 with IC_{50} vales ranging from 2.1 μM (TPC-010) to 16.7 μM (TPC-024) (Table 3, see Supporting Information Figures S10−S12). TPC-010 and TPC-011 showed similar inhibitory activity (IC_{50} = 2.1, 4.4 μM, respectively, Figure 5A,B) for NPP6, but they were not specific to NPP6 (Figure 5C). Among these compounds, we focused on TPC-009 because it efficiently (IC_{50} = 2.7 μM) and selectively inhibited NPP6 over other NPP family members (Figure 5C). In addition, TPC-009 has a suitable structure for chemical modification and is water-soluble.

Structure−Activity Relationship: Amine Substituents and Linker Length. To obtain more potent NPP6 inhibitors, we performed a structure−activity relationship (SAR) study of TPC-009. For this purpose, we focused on several compounds with similar structure to TPC-009, which had been included in

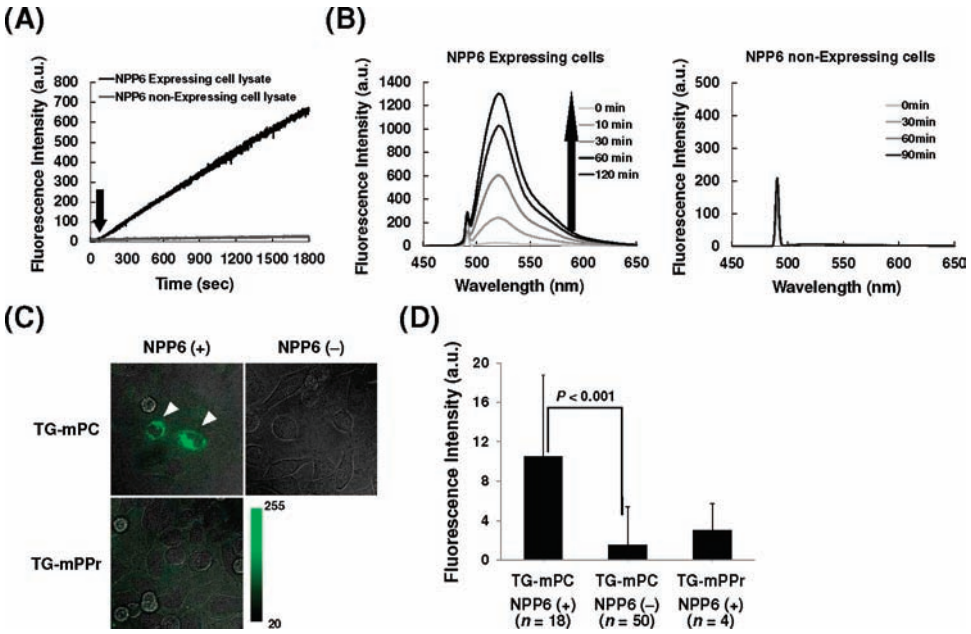

Figure 4. Cell-based assay with TG-mPC. (A) Cell lysate assay with TG-mPC. Cell lysate; NPP6 (+) NIH3T3 cell lysate, NPP6 (−) NIH3T3 cell lysate. The preparation of each lysate is described in Experimental Section. (B) Total NPP6 activity, i.e., membrane-associated and secreted NPP6 activity, of NPP6 (+) NIH3T3 cells and NPP6 (−) NIH3T3 cells. Excitation wavelength was 490 nm. (C) Fluorescence microscopic imaging of NPP6 activity in living cells with TG-mPC and TG-mPPr. HeLa cells expressing NPP6 or mock with mCherry were incubated with 10 μM solution of each probe in Hank's Balanced Salt Solution (HBSS) at 37 °C. Confocal fluorescence images and DIC images were captured at 3 min after addition of each probe. Arrowheads indicate NPP6 (+) HeLa cells. (D) Comparison of fluorescence intensities between NPP6 (+) and NPP6 (−) HeLa cells after addition of TG-mPC (final 10 μM) and TG-mPPr (final 10 μM). The results are mean ± SD.

Table 3. Inhibition (%) of NPP6 by Screening-Identified Compounds (TPC-009 to -011, and TPC-014 to -029, >50% inhibition at 10 μM) and the IC_{50} Values[c]

compound	IC_{50} (μM)	inhibition (%, at 10 μM in the screening)
TPC-009	2.7	96
TPC-010	2.1	92
TPC-011	4.4	62
TPC-014	6.7	54
TPC-015	4.3	76
TPC-016	–[a]	62
TPC-017	11.1	64
TPC-018	5.5	78
TPC-019	–[a]	55
TPC-020	5.6	71
TPC-021	5.0	66
TPC-022	9.8	74
TPC-023	4.5	53
TPC-024	16.7	50
TPC-025	11.1	60
TPC-026	5.9	62
TPC-027	16.2	55
TPC-028	3.9	88
TPC-029	–[b]	55

[a] No inhibitory activity (IC_{50} > 50 μM). [b] This compound shows fluorescence that interfered with the measurement of its IC_{50}, but it has inhibitory activity toward NPP6. [c] For the structures of TPC-014 to -029, see Supporting Information Figure S10.

the initial screening but had shown little or no inhibitory activity. Ten such compounds, named T1−T10 (Figure 6A), all had an isothiourea moiety as a partial structure. Among these compounds, T5 and T7 but not T1 inhibited NPP6. The rank order was T5 > T7 ≫T1 (Figure 6B). Thus, the linker length and the substituents of the amine moiety seem to be critical for the inhibitory activity. We therefore synthesized T11, which has a trimethylammonium group instead of the dimethylamino group in TPC-009 (see Supporting Information Scheme S2). T11 was found to be a potent and selective NPP6 inhibitor with an IC_{50} value of 0.21 μM (Figure 7A,B). Kinetic analysis revealed that T11 inhibits NPP6 in a competitive manner (Figure 7C). We also examined the effects of linker length and substituents of the amine moiety (primary amines, tertiary amines, and quaternary amines) on the inhibitory activity (Figure 8A,B). As a result, the length of linker, C_3, was found to be optimum. These experiments identified T11 as a potent NPP6 inhibitor with an optimum C_3 linker between the amine moiety and isothiourea moiety, and a favorable cationic trimethylammonium group.

Structure−Activity Relationship: Isothiourea Substituents. We also examined the substituents of isothiourea. The compounds we synthesized are shown in Figure 9A, and their IC_{50} values are summarized in Figure 9B. Isothiourea monosubstituted with moderate-sized substituents (methyl (T19), benzene (T16), and bis-(trifluoro)benzene (T17), but not naphthalene (T18)) showed inhibitory activity nearly identical to that of T11. On the other hand, disubstituted isothiourea compounds, such as dimethyl (T20), diethyl (T21), dibutyl (T22), cyEt (T23), and cyPr (T24), showed inhibitory activity lower than that of S11. However, trisubstituted

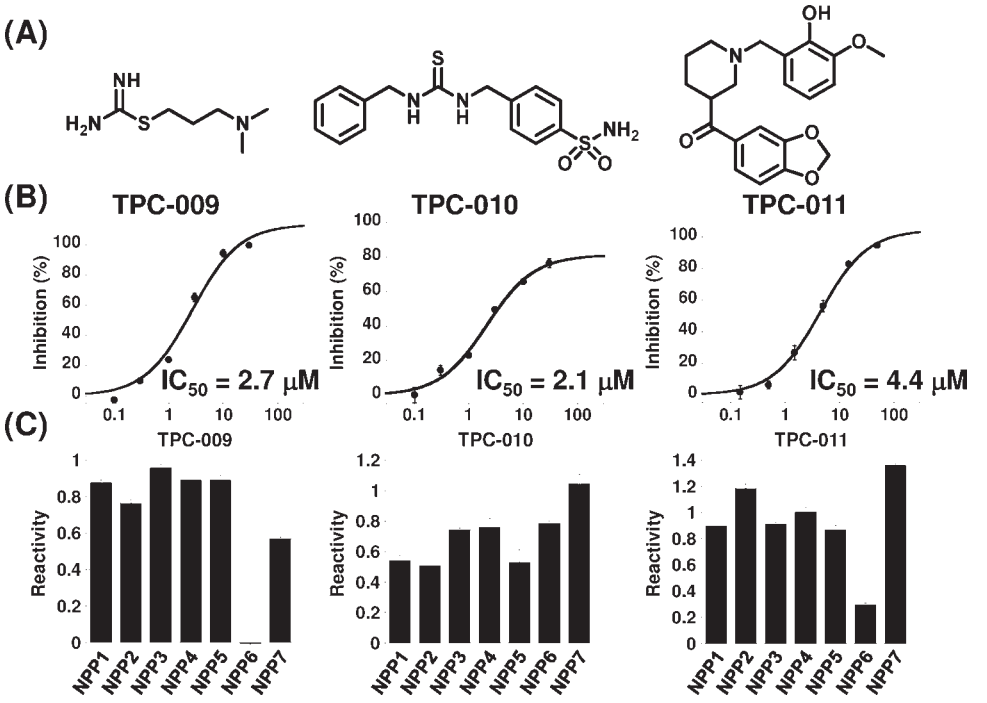

Figure 5. Inhibitory activity and selectivity of TPC-009, -010, -011 toward NPP6. (A) Structures of TPC-009, -010, -011, hit compounds in the primary screening. (B) Inhibition plots and curves of TPC-009, -010, -011. The IC_{50} values were 2.7, 2.1, 4.4 μM, respectively. The results are mean ± SD (n = 6). (C) Selectivity test of TPC-009, -010, -011 (50 μM) toward recombinant NPPs. The results are mean ± SD (n = 3). These values were determined by using absorption-based substrates, pNP-TMP (for NPP1−5) and pNPPC (for NPP6, -7) at 405 nm.

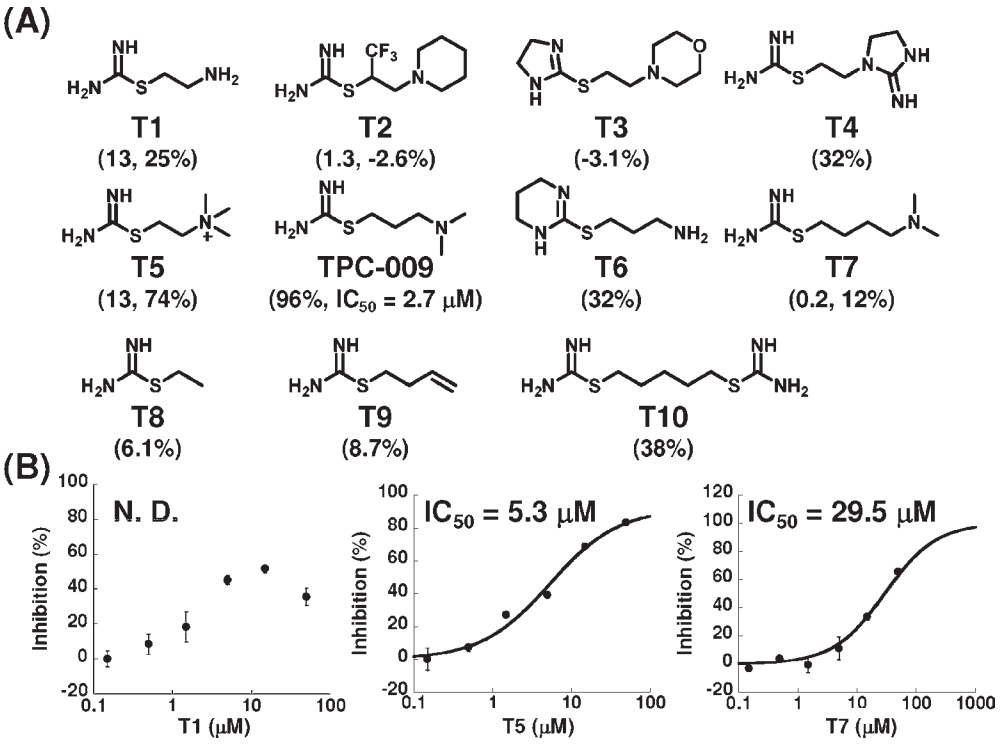

Figure 6. Inhibitory activity of primary screening samples toward NPP6. (A) Structures of TPC-009 and its analogues (T1−10) which showed low inhibitory activity in the primary screening. Inhibition (%) by the indicated compounds at 10 μM is shown in brackets. The inhibition (%) of T1, T2, T5, and T7 was measured twice. (B) Inhibition plots and curves of T1, T5, and T7 on the retest. IC_{50} values were >50 μM (N.D. = not determined), 5.3 μM, and 29.5 μM, respectively. The results are mean ± SD (n = 6).

dx.doi.org/10.1021/ja201028t |J. Am. Chem. Soc. 2011, 133, 12021–12030

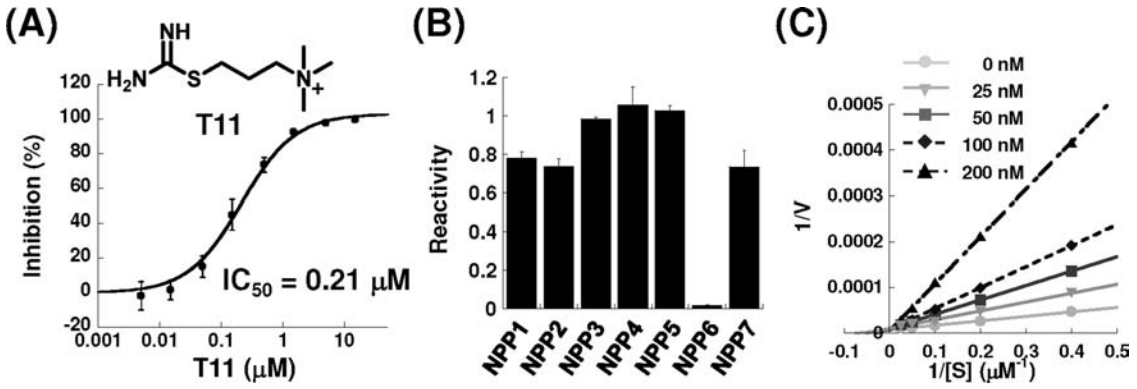

Figure 7. Inhibition plots and inhibition curve of T11 toward NPP6. (A) The IC_{50} value of T11 was 0.21 μM. The results are mean ± SD ($n = 6$). Inset: the structure of T11. (B) Selectivity test of T11 (50 μM) toward recombinant NPPs. The results are mean ± SD ($n = 3$). (C) Lineweaver−Burk plots of NPP6 inhibition, showing competitive inhibition by T11.

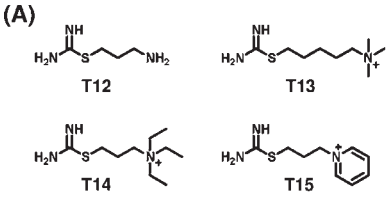

(B)

	primary	tertiary	quaternary		
	H, H	diMe	triMe	triEt	Py
n = 2	>30	–	5.3	–	–
n = 3	11	2.7	0.21	3.4	5.3
n = 4	–	30	–	–	–
n = 5	–	–	~100	–	–

Figure 8. T11 derivatives with various substituted amines and linker length (T12−15 and compounds in the primary screening). (A) Structures of T12−15. (B) IC_{50} values (μM) of the indicated compounds are shown. Synthesis of these compounds is shown in Scheme S3 (see Supporting Information).

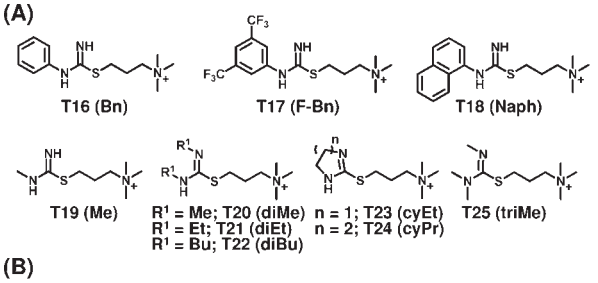

(B)

Compound	T16	T17	T18	T19	T20	T21	T22	T23	T24	T25
IC_{50} (μM)	0.27	0.17	1.5	0.59	1.9	6.2	16	5.1	11	0.22

Figure 9. T11 derivatives with substituted isothiourea (T16−25). (A) Structures of T16−25. T16−S19 are monosubstituted isothioureas, T20−24 are disubstituted isothioureas, and T25 is a trisubstituted isothiourea. (B) IC_{50} values of T11 derivatives with substituted isothioureas are shown. Synthesis of these compounds is shown in Scheme S4 (see Supporting Information).

isothiourea (trimethyl, T25) showed strong inhibitory activity, like that of T11.

CONCLUSION

The biological functions of NPP4−7 have not been elucidated in detail, and this fact led us to design and synthesize novel fluorescence probes for NPP6, i.e., TG-mPC and its derivatives, which were rationally designed as off/on type fluorescence probes based on the PeT mechanism. We anticipate that TG-mPC will be far more useful than previously reported NPP6 substrates, such as glycerophosphocholine (GPC), lysophosphatidylcholine (LPC), and *p*-nitrophenylphosphorylcholine (pNPPC), because it can detect NPP6 activity with high sensitivity and distinguish the activity of NPP6 from those of other NPP family members, including NPP2/autotaxin, as a consequence of our design strategy (for details, see Supporting Information Figure S1B,C and Figure 1). Previously reported probes, such as DDPB, could not distinguish between phospholipase D (PLD) and phospholipase C (PLC) activities.[33] Thus, TG-mPC is a novel, highly selective probe for lysoPLC (NPP6). Our strategy, as shown in Figure 1, in fact proved unnecessary, because it turned out that NPP2 did not hydrolyze TG-mPC, but nevertheless, this approach might be applicable to other enzymatic reactions, especially other phosphodiesterases that distinguish different cleavage sites.

Study of the reactivity of TG-mPC analogues with NPPs and the SAR of NPP6 inhibitors may also give us insight into the structure of NPP6. The recently solved NPP2 structure suggests that the difference of TG-mPC reactivity between NPP2 and NPP6 derives from the insertion loop, which is conserved in NPP family members except NPP2, in the proximity of the catalytic center.[43,44] Although the catalytic machinery is well conserved among the NPP family members, and they have a common native substrate, LPC, the substrate enters the catalytic pocket in opposite orientations in NPP2 and NPP6. Namely, the NPP2 catalytic pocket recognizes the fatty acid of LPC, while the NPP6 catalytic pocket recognizes the phosphorylcholine residue, and this determines the phosphodiester bond to be cleaved (lysoPLC vs lysoPLD). The phosphorylcholine residue in TG-mPC and its structural analogues are recognized by NPP6, and this may be the reason why they are NPP6-specific. It is noteworthy that TG-mPC discriminate between NPP6 and NPP7. Because previously reported colorimetric substrates do not discriminate these two

NPPs, TG-mPC appears to have another moiety that is specifically recognized by NPP6.

TG-mPC is also applicable to cell-based assay without interference from other enzymes, such as esterases and phosphatases (Figure 2C and see Supporting Information Figure S13). It was confirmed to be useful for cell-based NPP6 inhibitor screening and is expected to be suitable for real-time imaging of NPP6 activity in NPP6-expressing cells such as oligodendrocytes and kidney epithelial cells.[45] These projects are ongoing in our laboratory.

We found a potent and selective NPP6 inhibitor, T11 (Figures 5−9). Structure−activity relationship (SAR) analyses revealed that the structure of T11, which consists of trimethylammonium, propyl linker, and isothiourea, is optimum among the compounds synthesized in this study. We also examined the binding affinity of T11 for histamine receptors (H1−H4), inducible NOS (iNOS), and constitutive NOS (cNOS), and the inhibitory activity toward acetylcholinesterase (AchE) (see Supporting Information Figure S14). T11 showed inhibitory activity toward H4 receptor at 10 μM (about 50% inhibition) but had no effect on the other enzymes. Our proposed inhibition mechanism of T11 is shown in Figure S15 (see Supporting Information). T11 has a similar structure to LPC, i.e., a natural substrate of NPP6. The trimethylammonium group is common, and a chelating moiety for Zn^{2+} is seen in both structures: phosphate group for LPC and isothiourea moiety for T11. In this report, we especially focused on the structure of TPC-009; however, other compounds may be still valuable as lead compounds of highly potent NPP6-selective inhibitors. For instance, it is considered that TPC-011, which has a scaffold different from that of TPC-009, may be an attractive candidate as an NPP6 inhibitor, because it has comparatively potent inhibitory activity and high selectivity for NPP6. Moreover, we have already examined the SAR of TPC-011 (see Supporting Information Figure S16). Although the results are not entirely clear-cut, TPC-011 derivatives may prove to be potent and selective NPP6 inhibitors.

In summary, we have developed a novel fluorescence probe, TG-mPC, which can selectively detect NPP6/lysophospholipase C activity, and especially, distinguish NPP6 from NPP2/lysophospholipase D based on our rational design strategy. We confirmed that it can be utilized in cellular systems. We think that TG-mPC will be useful to elucidate the function of NPP6, because it is the first NPP6-selective probe. We also found a novel and potent NPP6-selective inhibitor, T11. We believe that T11 cannot only contribute to the elucidation of NPP6 function as an alternative to knockout mice or RNAi but also may have wider application, e.g., in the development of candidate therapeutic agents for treatment of NPP6-related diseases, because it is the first-in-class NPP6 inhibitor.[46−49]

EXPERIMENTAL SECTION

Materials. ALP was purchased from Sigma-Aldrich Japan. *p*-Nitrophenylthymidine 5′-monophosphate (pNP-TMP) and *p*-nitrophenylphosphorylcholine (pNPPC) were purchased from Sigma. All other reagents and solvents listed below or described in the legend to each synthetic scheme were purchased from Tokyo Kasei Co., Ltd. (Japan), Wako Pure Chemical Industries, Ltd. (Japan), or Aldrich Chemical Co. Dehydrated DMF, methanol, ethanol, dichloromethane, and pyridine were 99% purity or greater. Unless otherwise specified, reagents were of the lowest acceptable grade and were used without further purification. ^{1}H NMR spectra were recorded on JEOL JNM-LA300 and JEOL JNM-LA400 instruments; δ values are given in ppm from the solvent resonance as the internal standard. Data are reported as follows: chemical shift, multiplicity (*s* = singlet, d = doublet, t = triplet, br = broad, and m = multiplet), integration, and *J* coupling. Mass spectra were recorded on a JEOL JMS-T100LC mass spectrometer. Silica gel column chromatography was performed using silica gel 60 (Kanto Chemical Co., Inc., Japan) and Chromatorex-NH silica gel (Fuji Silysia Chemical, Kasugai, Japan). Preparative HPLC purification was performed on a reverse-phase ODS column (GL Sciences, Japan, Inertsil ODS-3 10 mm × 250 mm) using 0.1% trifluoroacetic acid in water as eluent A and 0.1% trifluoroacetic acid, 80% acetonitrile, and 20% water as eluent B, or 100 mM TEAA in water as eluent A and 80% acetonitrile, and 20% water as eluent B, with a JASCO PU-2080 plus system, at a flow rate of 5.0 mL/min. HPLC analyses were performed on a reversed-phase ODS column (GL Sciences, Inertsil ODS-3 4.6 mm × 250 mm), fitted on a JASCO PU-980 plus system, at a flow rate of 1.0 mL/min. UV−visible spectra were obtained on a Shimadzu UV-1600 (Tokyo, Japan). Fluorescence spectra were obtained on a Hitachi F4500 (Tokyo, Japan). Fluorescence assay on 384-well plates were performed using Perkin-Elmer EnVision Multilabel Plate Readers (Beaconsfield, Buckinghamshire, England) or PHERAstar (BMG LABTECH, Germany)

Determination of Kinetic Parameters. Various concentrations of probes (TG-mPC, TG-mPC$_3$C, pNPPC, and CPF4) were dissolved in NPP buffer (100 mM Tris-HCl buffer (pH 9.0), containing 500 mM NaCl, 5 mM $MgCl_2$, and 0.05% Triton-X100). NPP6 or NPP2 was added to the solution, and the fluorescence intensity was recorded continuously. Initial reaction velocity was calculated and plotted against probe concentration, and the points were fitted to a Michaelis−Menten curve. K_m and V_{max} were determined by the least-squares method.

HPLC Analysis. To confirm that the enzymatic reaction took place, reversed-phase HPLC analysis was performed using an Inertsil 3 ODS column (4.6 mm × 250 mm, GL Science, Japan), fitted on a JASCO PU980 HPLC system. Conditions and recorded absorption wavelength are given in the figure legends.

Fluorometric Analysis. The slit width was 2.5 nm for both excitation and emission. The photomultiplier voltage was 750 V. TG-Phos, TG-mPC, TG-mPhos, and TG-mPC analogues were dissolved in NPP buffer to obtain 500 μM stock solutions. Relative fluorescence quantum yields (Φ_{Fl}) were obtained by comparing the area under the emission spectrum of the probes with that of a solution of fluorescein (Φ_{Fl} = 0.85) in aq 0.1 N NaOH.

ALP, PLE, and AchE Assay. ALP assay was performed in ALP buffer (50 mM Tris-HCl buffer (pH 8.0), containing 0.5 mM $MgCl_2$). PLE assay was performed in 100 mM sodium phosphate buffer (pH 7.4) at room temperature. AchE assay was performed in phosphate-buffered saline (PBS, pH 7.4) at room temperature.

NPP6 Inhibitor Screen. High-throughput screening (HTS) was performed against a part of the chemical library (80 000 compounds) of the Chemical Biology Research Initiative, The University of Tokyo. Screening methods were as follows; at first, small molecules (2 mM DMSO stock solution) from library plates (320 compounds/384 wells) were diluted with NPP buffer to 30 μM solution (1.5% DMSO) by the Multi-Dispensor EDR 384 (BioTec, Japan). Next, TG-mPC (1.5 μM, no DMSO) solution (5 μL) was dispensed into the individual wells of the assay plates, and the prepared solution (5 μL) of compounds was also added into each well. Finally, NPP6 solution (5 μL) was dispensed into the plates (total volume was 15 μL), and the plates were incubated at room temperature for 60 min. The fluorescence of 2-Me-4-OMe TG was measured (λ_{ex} = 490 nm, λ_{em} = 510 nm) for all plates by a microplate reader. Background control wells (i.e., no enzyme wells, n = 4) were also prepared for all plates.

Analysis of the Inhibitor Screening. Inhibition (%) of all samples was calculated by use of the following eq A.

$$\text{inhibition}\ (\%) = 100 \times [(\text{FI}_{\text{sample}} - \text{FI}_{\text{background}})/(\text{FI}_{\text{median}} - \text{FI}_{\text{background}})] \quad \text{(A)}$$

where FI_{sample} is the fluorescence intensity of the sample, $FI_{background}$ is the average fluorescence intensity of four background control samples, and FI_{median} is the average fluorescence intensity of two median samples from each plate (320 samples).

Selectivity Test. Inhibitory activity of the hit compounds toward NPP1−7 was calculated using pNP-TMP (for NPP1−5) and pNPPC (for NPP6, -7). The final concentration of these two absorption-based substrates was 100 μM. Assay protocol was as follows: assay buffer (NPP buffer, 37 μL) was dispensed into a 96-well microplate and 500 μM pNP-TMP or pNPPC (20 μL) was dispensed into the microplate. Then, 30 μM samples (33 μL) were added, and finally NPP1−7 solution (10 μL) was added to each well. Total volume of each well was 100 μL. The plate was incubated for 2 h, and absorbance (405 nm) was measured by a microplate reader.

Preparation of Recombinant NPPs. Recombinant NPPs were prepared as follows. HEK293 cells were cultured in Dulbecco's modified Eagle's medium (DMEM) supplemented with antibiotics, glutamine, and 10% fetal bovine serum under an atmosphere of 5% CO_2 at 37 °C. HEK293 cells were transfected with the cDNAs using Lipofectamine 2000 reagent (Invitrogen) according to the manufacturer's protocol. Cell culture media were collected 48 h after the transfection. Collected culture media of all NPPs were used without further purification.

Cell-Based Assays. NPP6-expressing NIH3T3 cells and nonexpressing NIH3T3 cells were cultured in DMEM supplemented with penicillin (100 units/mL), streptomycin (100 μg/mL), glutamine, and 10% fetal bovine serum in a humidified incubator containing 5% CO_2 gas at 37 °C. Lysates of NPP6-expressing NIH3T3 cells and nonexpressing cells were prepared with CelLyticTMM (Sigma-Aldrich) according to the manufacturer's protocol.

Preparation of Cells for Fluorescence Imaging. Cells were grown on a PDL-coated 35 mm diameter glass-bottomed dish (MatTek; Ashland). HeLa cells were transfected with NPP6 and mCherry plasmids by the use of Lipofectamine LTX and Plus Reagent (Invitrogen) 1 day before imaging.

Fluorescence Imaging. Confocal fluorescence images were taken with a TCS SP-5 (Leica), where appropriate LASER and filter sets were chosen for each fluorescence color as indicated. Fluorescence imaging was performed in Hank's Balanced Salt Solution (HBSS) at 37 °C, unless otherwise stated.

■ ASSOCIATED CONTENT

Ⓢ Supporting Information. Synthesis description, supporting figures, and complete references. This material is available free of charge via the Internet at http://pubs.acs.org.

■ AUTHOR INFORMATION

Corresponding Author
tlong@mol.f.u-tokyo.ac.jp

Notes
[†]Abbreviations used: NPP, nucleotide pyrophosphatase/phosphodiesterase; lysoPLC, lysophosholipase C; lysoPLD, lysophosholipase D; LPC, lysophoshitidylcholine; SM, sphingomyelin; GPC, glycerophoshorylcholine; pNP-TMP, *p*-nitrophenylthymidine 5′-monophosphate; pNPPC, *p*-nitrophenylthymidine-phoshorylcholine; FAAH, fatty acid amide hydrolase; ALP, alkaline phosphatase; PLE, porcine liver esterase; AChE, acetylcholine esterase; NOS, nitric oxide synthase; TG, TokyoGreen; TG-mPC, methylenoxyphosphorylcholine; PeT, photoinduced electron transfer; HTS, high-throughput screening; SAR, structure−activity relationship.

■ ACKNOWLEDGMENT

This work was supported in part by the Ministry of Education, Culture, Sports, Science and Technology of Japan (grant nos. 22000006 to T.N., 20689001 and 21659024 to K.H., and 21750135 to T.T.), and by a grant from the Industrial Technology Development Organization (NEDO) of Japan (to T.T.). K.H. was also supported by Sankyo Foundation of Life Science, and M.K. was supported by a Grant-in-Aid for JSPS Fellows. This work was supported in part by funds from the Target Protein Research Programs from the Ministry of Education, Culture, Sports, Science and Technology of Japan.

■ REFERENCES

(1) Bollen, M.; Gijsbers, R.; Ceulemans, H.; Stalmans, W.; Stefan, C. *Crit. Rev. Biochem. Mol. Biol.* **2000**, *35*, 393–432.
(2) Goding, J. W.; Grobben, B.; Slegers, H. *Biochim. Biophys. Acta* **2003**, *1638*, 1–19.
(3) Sakagami, H.; Aoki, J.; Natori, Y.; Nishikawa, K.; Kakehi, Y.; Natori, Y.; Arai, H. *J. Biol. Chem.* **2005**, *280*, 23084–23093.
(4) Duan, R.-D.; Bergman, T.; Xu, N.; Wu, J.; Cheng, Y.; Duan, J.; Nelander, S.; Palmberg, C.; Nilsson, A. *J. Biol. Chem.* **2003**, *278*, 38528–38536.
(5) Deterre, P.; Gelman, L.; Gary-Gouy, H.; Arrieumerlou, C.; Berthelier, V.; Tixier, J. M.; Ktorza, S.; Goding, J.; Schmitt, C.; Bismuth, G. *J. Immunol.* **1996**, *157*, 1381–1388.
(6) Scott, L. J.; Delautier, D.; Meerson, N. R.; Trugnan, G.; Goding, J. W.; Maurice, M. *Hepatology* **1997**, *25*, 995–1002.
(7) Johnson, K.; Hashimoto, S.; Lotz, M.; Pritzker, K.; Goding, J.; Terkeltaub, R. *Arthritis Rheum.* **2001**, *44*, 1071–1081.
(8) Huang, R.; Rosenbach, M.; Vaughn, R.; Provvedini, D.; Rebbe, N.; Hickman, S.; Goding, J.; Terkeltaub, R. *J. Clin. Investig.* **1994**, *94*, 560–567.
(9) Johnson, K.; Moffa, A.; Chen, Y.; Pritzker, K.; Goding, J.; Terkeltaub, R. *J. Bone Miner. Res.* **1999**, *14*, 883–892.
(10) Whitehead, J. P.; Humphreys, P. J.; Dib, K.; Goding, J. W.; O'Rahilly, S. *Clin. Endocrinol.* **1997**, *47*, 65–70.
(11) Belfiore, A.; Costantino, A.; Frasca, F.; Pandini, G.; Mineo, R.; Vigneri, P.; Maddux, B.; Goldfine, I. D.; Vigneri, R. *Mol. Endocrinol.* **1996**, *10*, 1318–1326.
(12) Maddux, B. A.; Sbraccia, P.; Kumakura, S.; Sasson, S.; Youngren, J.; Fisher, A.; Spencer, S.; Grupe, A.; Henzel, W.; Stewart, T. A.; Reaven, G. M.; Goldfine, I. D. *Nature* **1995**, *373*, 448–451.
(13) Abate, N.; Chandalia, M.; Di Paola, R.; Foster, D. W.; Grundy, S. M.; Trischitta, V. *Nat. Clin. Pract. Endocrinol. Metab.* **2006**, *2*, 694–701.
(14) Nam, S. W.; Clair, T.; Kim, Y. S.; McMarlin, A.; Schiffmann, E.; Liotta, L. A.; Stracke, M. L. *Cancer Res.* **2001**, *61*, 6938–6944.
(15) Inoue, M.; Ma, L.; Aoki, J.; Chun, J.; Ueda, H. *Mol. Pain* **2008**, *4*, 6–10.
(16) Kano, K.; Ariyama, N.; Ohgami, M.; Aoki, J. *Curr. Med. Chem.* **2008**, *15*, 2122–2131.
(17) Nakasaki, T. *Am. J. Pathol.* **2008**, *173*, 1566–1576.
(18) Nam, S. W.; Clair, T.; Campo, C. K.; Lee, H. Y.; Liotta, L. A.; Stracke, M. L. *Oncogene* **2000**, *19*, 241–247.
(19) Nakagawa, K.; Hama, K.; Aoki, J. *J. Boichem.* **2010**, *148*, 13–24.
(20) Takakusa, H.; Kikuchi, K.; Urano, Y.; Sakamoto, S.; Yamaguchi, K.; Nagano, T. *J. Am. Chem. Soc.* **2002**, *124*, 1653–1657.
(21) van Meeteren, L. A.; Ruurs, P.; Christodoulou, E.; Coding, J. W.; Takakusa, H.; Kikuchi, K.; Perrakis, A.; Nagano, T.; Moolenaar, W. H. *J. Biol. Chem.* **2005**, *280*, 21155–21161.
(22) Ferguson, C. G.; Bigman, C. S.; Richardson, R. D.; van Meeteren, L. A.; Moolenaar, W. H.; Prestwich, G. D. *Org. Lett.* **2006**, *8*, 2023–2026.
(23) Umezu-Goto, M.; Kishi, Y.; Taira, A.; Hama, K.; Dohmae, N.; Takio, K.; Yamori, T.; Mills, G. B.; Inoue, K.; Aoki, J.; Arai, H. *J. Cell Biol.* **2002**, *158*, 227–233.
(24) Tokumura, A.; Majima, E.; Kariya, Y.; Tominaga, K.; Kogure, K.; Yasuda, K.; Fukuzawa, K. *J. Biol. Chem.* **2002**, *277*, 39436–39442.

(25) Boutin, J. A.; Ferry, G. *Cell. Mol. Life Sci.* **2009**, *66*, 3009–3021.
(26) van Meeteren, L. A.; Moolenaar, W. H. *Prog. Lipid Res.* **2007**, *46*, 145–160.
(27) Saunders, L. P.; Ouellette, A.; Bandle, R.; Chang, W. C.; Zhou, H.; Misra, R. N.; De La Cruz, E. M.; Braddock, D. T. *Mol. Cancer Ther.* **2008**, *7*, 3352–3362.
(28) Hoeglund, A. B.; Bostic, H. E.; Howard, A. L.; Wanjala, I. W.; Best, M. D.; Baker, D. L.; Parrill, A. L. *J. Med. Chem.* **2010**, *53*, 1056–1066.
(29) Albers, H. M. H. G.; Dong, A.; van Meeteren, L. A.; Egan, D. A.; Sunkara, M.; van Tilburg, E. W.; Schuurman, K.; van Tellingem, O.; Morris, A. J.; Smyth, S. S.; Moolenaar, W. H.; Ovaa, H. *Proc. Natl. Acad. Sci. U.S.A.* **2010**, *107*, 7257–7262.
(30) Gierse, J.; et al. *J. Pharmacol. Exp. Ther.* **2010**, *334*, 310–317.
(31) Mulder, A. M.; Cravatt, B. F. *Biochemistry* **2006**, *45*, 11267–11277.
(32) Macarron, R.; Banks, M. N.; Bojanic, D.; Burns, D. J.; Cirovic, D. A.; Garyantes, T.; Green, D. V.; Hertberg, R. P.; Janzen, W. P.; Paslay, J. W.; Schopfer, U.; Sittampalam, G. S. *Nat. Rev. Drug Discovery* **2011**, *10*, 188–195.
(33) Rose, T. M.; Prestwich, G. D. *Org. Lett.* **2006**, *8*, 2575–2578.
(34) Haung, W.; Hicks, S. N.; Sondek, J.; Zhang, Q. *ACS Chem. Biol.* **2011**, *6*, 223–228.
(35) Gonzalez, O. A.; Mombru, A. W.; Suescun, L. P.; Mariezcurrena, R. A.; Manta, E.; Prandi, C. *Acta Crystallogr., Sect. C: Cryst. Struct. Commun.* **1996**, *C52*, 2875–2878.
(36) Velazquez, C. A.; Chen, Q.-H.; Citro, M. L.; Keefer, L. K.; Knaus, E. E. *J. Med. Chem.* **2008**, *51*, 1954–1961.
(37) Urano, Y.; Kamiya, M.; Kanda, K.; Ueno, T.; Hirose, K.; Nagano, T. *J. Am. Chem. Soc.* **2005**, *127*, 4888–4894.
(38) Kamiya, M.; Kobayashi, H.; Hama, Y.; Koyama, Y.; Bernardo, M.; Nagano, T.; Choyke, P. L.; Urano, Y. *J. Am. Chem. Soc.* **2007**, *129*, 3918–3929.
(39) Kamiya, M.; Urano, Y.; Ebata, N.; Yamamoto, M.; Kosuge, J.; Nagano, T. *Angew. Chem., Int. Ed.* **2005**, *44*, 5439–5441.
(40) Mantyla, A.; Vepsalainen, J.; Jarvinen, T.; Nevalainen, T. *Tetrahedron Lett.* **2002**, *43*, 3793–3794.
(41) Fleisher, D.; Bong, R.; Stewart, B. H. *Adv. Drug Delivery Rev.* **1996**, *19*, 115–130.
(42) Krise, J. P.; Stella, V. J. *Adv. Drug Delivery Rev.* **1996**, *19*, 287–310.
(43) Nishimasu, H.; Okudaira, S.; Hama, K.; Mihara, E.; Dohmae, N.; Inoue, A.; Ishitani, R.; Takagi, J.; Aoki, J.; Nureki, O. *Nat. Struct. Mol. Biol.* **2011**, *18*, 205–212.
(44) Hausmann, J.; et al. *Nat. Struct. Mol. Biol.* **2011**, *18*, 198–204.
(45) Willmann, J. K.; van Bruggen, N.; Dinkelborg, L. M.; Gambhir, S. S. *Nat. Rev. Drug Discovery* **2008**, *7*, 591–607.
(46) Nixon, G. F.; Mathieson, F. A.; Hunter, I. *Prog. Lipid Res.* **2008**, *47*, 62–75.
(47) Schmitz, G.; Ruebsaamen, K. *Atherosclerosis* **2010**, *208*, 10–18.
(48) Lee, H. C.; Fellenz-Maloney, M. P.; Liscovitch, M. *Proc. Natl. Acad. Sci. U.S.A.* **1993**, *90*, 10086–10090.
(49) Hartmann, T.; Kuchenbecker, J.; Grimm, M. O. W. *J. Neurochem.* **2007**, *103*, 159–170.